

Aggregation of magnetic holes in a rotating magnetic field

Jozef Černák,

*P. J. Šafárik University in Košice, Institute of Physics,
Jesenná 5, SK-04000 Košice, Slovak Republic **

Geir Helgesen,

Institute for Energy Technology, Physics Department, NO-2027, Kjeller, Norway

Abstract

We have experimentally investigated field induced aggregation of nonmagnetic particles confined in a magnetic fluid layer when rotating magnetic fields were applied. After application of a magnetic field rotating in the plane of the fluid layer, the single particles start to form two-dimensional (2D) clusters, like doublets, triangles, and more complex structures. These clusters aggregated again and again to form bigger clusters. During this nonequilibrium process, a broad range of cluster sizes was formed, and the scaling exponents, z and z' , of the number of clusters $N(t) \sim t^{z'}$ and average cluster size $S(t) \sim t^z$ were calculated. The process could be characterized as diffusion limited cluster-cluster aggregation. We have found that all sizes of clusters that occurred during an experiment, fall on a single curve as the dynamic scaling theory predicts. However, the characteristic scaling exponents z' , z and crossover exponents Δ were not universal. A particle tracking method was used to find the dependence of the diffusion coefficients D_s on cluster size s . The cluster motions show features of Brownian motion. The average diffusion coefficients $\langle D_s \rangle$ depend on the cluster sizes s as a power law $\langle D_s \rangle \propto s^\gamma$ where values of γ as different as $\gamma = -0.62 \pm 0.19$ and $\gamma = -2.08 \pm 0.51$ were found in two of the experiments.

PACS numbers: 83.10.Tv, 75.50.Mm, 82.70.Dd, 89.75.Da

*Electronic address: jozef.cernak@upjs.sk

I. INTRODUCTION

Colloidal aggregation phenomena are interesting subjects of study for both theoretical and technological reasons. In systems with short range interactions the main aggregation features are well understood (**author?**) [1]. Diffusion limited cluster-cluster aggregation (CCA) model (**author?**) [2, 3] and dynamic scaling theory (**author?**) [4] explain well the scaling properties during aggregation. It was found that these models, initially developed for systems with short range interactions, can be used in systems where dipole-dipole interaction is dominant, for example aggregation of magnetic microspheres (**author?**) [5, 6], aggregation of nanoparticles in magnetic fluid (**author?**) [7] and aggregation of magnetic holes (**author?**) [8]. These experimental results show scaling of the significant parameters and features typical of CCA. On the other hand, the corresponding exponents may deviate slightly from the known models, and the reasons for this is still not understood.

Our previous results (**author?**) [8] served as motivation for this study. Aggregation of magnetic holes in constant magnetic fields was interpreted in frames of the CCA model and dynamic scaling theory. The scaling exponent $z \approx 0.42$ for the cluster size dependence $S(t) \sim t^z$ was found for particles of diameters $d = 1.9$ and $4\mu\text{m}$. This value of the exponent is slightly lower than exponent values predicted by theory ($z = 0.5$) (**author?**) [2] or exponents found by computer simulations ($z = 0.5$ for isotropic and $z = 0.61$ for anisotropic aggregation) (**author?**) [9]. Under certain experimental conditions (i.e., particles with larger diameter $d = 14\mu\text{m}$) the exponent z was close to or lower than the exponent value corresponding to a transition from 2D aggregation to 1D aggregation ($z = 1/3$). Based on these optical observations we know that for a constant magnetic field clusters move in 2D but they grow only in one dimension.

The constant magnetic fields induced formation of long chains of particles (**author?**) [6, 8]. To determine correct scaling exponents we may take into account hydrodynamic effects (**author?**) [9]. We proposed to apply rotating magnetic fields to ensure quasi isotropic properties inside the magnetic fluid (MF) sample. In this case clusters can move in 2D space and can grow as 2D compact objects and thus the hydrodynamic correction is less important.

The dynamic properties of a few magnetic holes (**author?**) [10] in rotating magnetic fields show interesting phenomena, for example nonlinear response of bound pairs of magnetic holes (**author?**) [11], complex braid dynamics (**author?**) [12], and equilibrium configurations

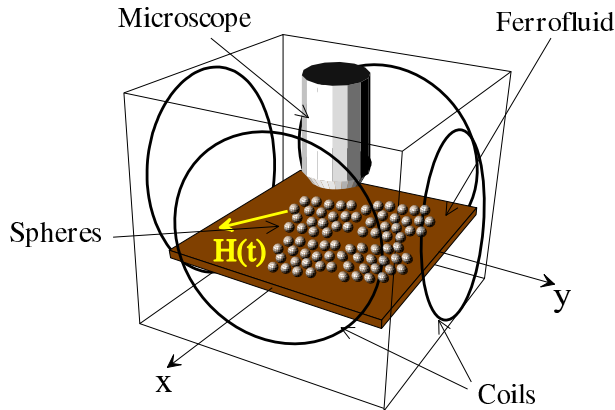


FIG. 1: (colour online) Experimental setup used to study aggregation of magnetic holes. A rotating magnetic field $\mathbf{H}(t)$ is applied in the plane of the magnetic fluid.

of rotating particles without contact between particles (**author?**) [13]. In a precessing magnetic field paramagnetic particles dispersed in a drop of water self-assemble into two-dimensional viscoelastic small clusters (**author?**) [14].

In the present study field induced aggregation of many magnetic holes has been observed. In Sec. II the experimental equipment and the methods used are described. The Sec. III deals with the results concerning the determination of the scaling exponents and characterization of the diffusion behaviour of individual clusters by tracking of their motions. In Sec. IV we summarize the general features and try to explain the non-universal scaling exponents. Our conclusions follow in Sec. V.

II. MICROSCOPIC OBSERVATIONS

The experimental setup shown in Fig. 1 consists of an optical microscope (Nikon Optiphot), two pairs of coils, and a carefully prepared thin layer sample. Alternating currents were supplied to the coils in order to produce a magnetic field rotating in the horizontal plane of the sample. Microscopic observations were captured by a CCD camera (Q-Imaging Micropublisher 5) with resolution 2560×1920 pixels.

The sample size was about $20 \times 20 \text{ mm}^2$. A layer of magnetic fluid of thickness approximately $50 \mu\text{m}$ was confined between two glass plates and sealed. The kerosene based magnetic fluid (**author?**) [15] had the following physical properties: density $\rho = 1020 \text{ kgm}^3$, susceptibility $\chi = 0.8$, saturation magnetization $M_s = 20\text{mT}$, and viscosity $\eta = 6 \times 10^3 \text{ Nsm}^2$.

Monodisperse polystyrene microspheres of diameter $d = 3\mu\text{m}$ were dispersed in the MF layer in order to create magnetic holes in presence of magnetic fields.

Without a magnetic field the particles are homogeneously dispersed in the layer and they can move freely. After some time a very low fraction of particles may randomly join to other particles and a few dimers were observed (**author?**) [10]. Their volume fraction is very low in comparison with the volume fraction of single particles. However, before the application of the rotating magnetic field, a short magnetic field pulse perpendicular to the sample (coils are not shown in Fig. 1) was applied in order to destroy these dimers and to create a monodisperse initial size distribution of particles. This initial stage of the experiment is not shown in Fig. 2.

The rotating magnetic field $\mathbf{H}(t) = (H_x, H_y)$ within the $x - y$ plane had the components: $H_x = H \sin(\omega t)$ and $H_y = H \sin(\omega t + \pi/2)$. The amplitude of the magnetic field was constant $H = 793 \text{ Am}^{-1}$, and angular velocity $\omega = 251 \text{ s}^{-1}$. The temperature during the experiments was $T \doteq 293 \text{ K}$. The effective volume susceptibility including the demagnetization correction for spherical magnetic holes was $\chi_{eff} = \chi/(1 + 2\chi/3) = 0.63$. The dimensionless interaction strength parameter (**author?**) [8] was $\lambda \doteq 90$. Here, $\lambda = U_{max}^{dip}/kT$, where U_{max}^{dip} is maximal dipolar energy of two joined dipolar particles, k is Boltzmann's constant and T is the temperature. Thus, dipole-dipole interaction among magnetic holes was dominant over the thermal fluctuations.

The rotating magnetic field induced an aggregation of the microspheres. The process took place via the joining of single particles into dimers, trimers and formation of 2D clusters consisting of many particles. These new clusters aggregate again and formed bigger clusters. A typical aggregation dynamics is shown in Fig. 2. A few samples with approximately the same layer thickness were investigated. The volume fractions of particles were low, in the range $\phi = 0.0014 - 0.0064$.

In order to analyze the digital images, a C programming language code and open graphical libraries were used. Several thousands of digital pictures have been analyzed in a distributed manner in a computational grid. We have analyzed the motion of individual particles during aggregation using our own tracking algorithms written in the Python programming language. The main advantage of the algorithm that was used is that it can track positions of new clusters which are results of the aggregation.

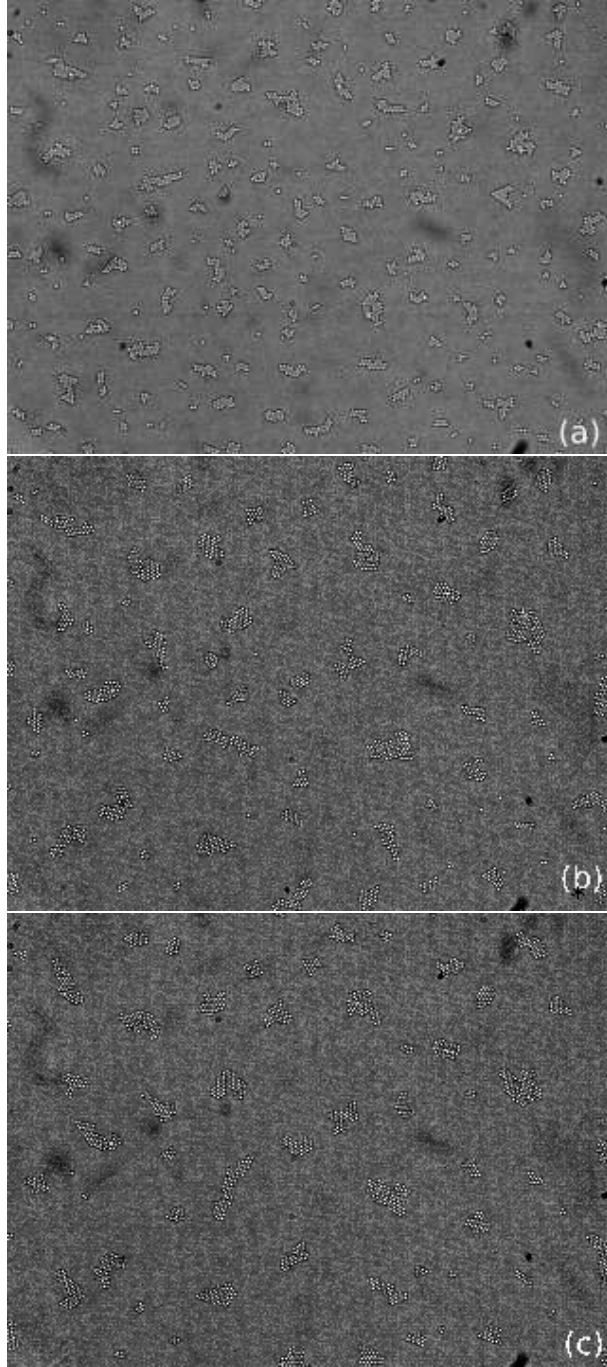


FIG. 2: Optical micrographs of aggregation of nonmagnetic microspheres with diameter $d = 3\mu\text{m}$ in magnetic fluid at different times: (a) $t = 600$ s, (b) $t = 3000$ s, and (c) $t = 3400$ s after the magnetic field was switched on. The applied rotating magnetic field had an amplitude $|\mathbf{H}| = 793$ Am^{-1} and frequency $f = 40$ Hz. The optical view covers a sample area of about $368\mu\text{m} \times 274\mu\text{m}$.

III. RESULTS

Microspheres inside a magnetic fluid layer without magnetic field behave as nonmagnetic particles dispersed in fluid. They perform random Brownian motion. In this case, aggregation events are rare due to the low particle concentration. Thus, in the initial stage of the experiments the microspheres are homogeneously dispersed in the layer of MF and the cluster size distribution is unimodal.

After application of the external magnetic field the microspheres begin to behave as interacting magnetic dipoles. They have induced magnetic moments which are oppositely oriented to the external magnetic field. When the energy of dipole-dipole interaction among two arbitrary spheres is larger than the thermal energy of the spheres, as quantified by the dimensionless interaction strength $\lambda \doteq 90$ in the present case, field induced aggregation starts.

During the aggregation complex motions of microspheres and clusters consisting of many microspheres were observed. Clusters containing regularly ordered particles were formed and small irregular clusters relatively quickly relax to highly ordered structures. Based on the optical observation the complex modes of motion of microspheres and clusters may be classified as; i) joining of two clusters together followed by a very slow relaxation of the microspheres in the new cluster into a more ordered structure; ii) extremely slowly swivelling of all clusters in the same direction as the rotating magnetic field, followed by packing into a compact disk form; and iii) small random motions of the clusters induced by random forces resulting from interactions with the local cluster environment.

We have observed that clusters of all sizes can join together and form bigger cluster which is the basic feature of cluster-cluster aggregation. The cluster-cluster aggregation model (author?) [2] predicts the scaling properties of the total number of clusters $N(t)$ and mean cluster size $S(t)$. The total number of clusters is defined as $N(t) = \sum_s n_s(t)$ where $n_s(t)$ is number of clusters of size s at time t . The mean cluster size $S(t)$ is defined as:

$$S(t) = \frac{\sum_s n_s(t) s^2}{\sum_s n_s(t) s} \quad (1)$$

where s is cluster size. In our case the cluster size s is given by the number of particles which belong to the cluster.

The aggregation process in Fig. 2 was studied in more details. In Fig. 3 (a) we can

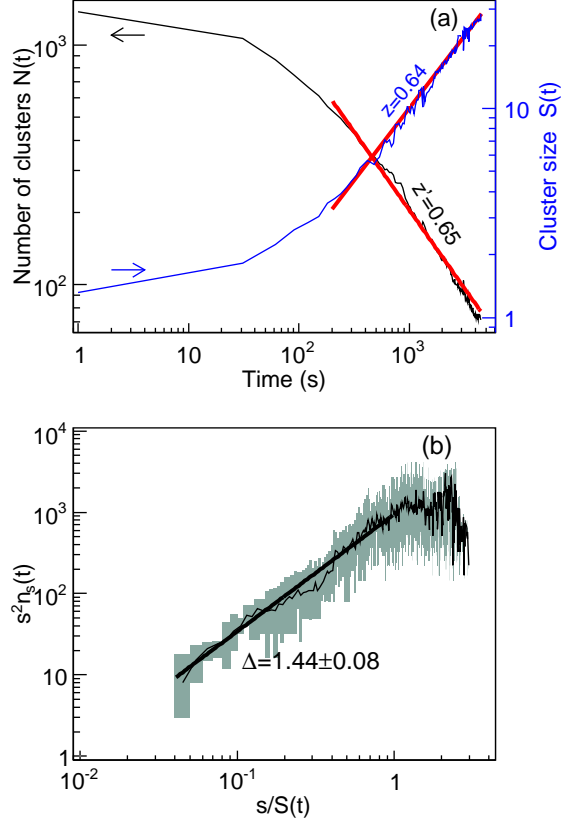


FIG. 3: (color online) (a) The total number of clusters $N(t)$ and the mean (weight average) cluster size $S(t)$ [in units of number of spheres] versus time. (b) The scaling function $g(x) = s^2 n_s(t)$ obtained from the cluster size distributions $n_s(t)$ during the time interval $t = 200 - 3400$ s.

see that the total number of clusters $N(t)$ and mean cluster size $S(t)$ show power law dependencies $N(t) \sim t^{z'}$ and $S(t) \sim t^z$. The power-law behaviour was found for the time interval $t = 200 - 3400$ s. The scaling exponents were determined as $z' = 0.65 \pm 0.01$ and $z = 0.64 \pm 0.01$.

Based on dynamic scaling theory (**author?**) [4] all number of clusters $n_s(t)$ observed during aggregation can be scaled into a single, universal curve or scaling function $g(x)$ defined as:

$$n_s(t) \sim s^{-2} g(s/t^z). \quad (2)$$

It is expected that $g(x) \sim x^\Delta$ for $x \ll 1$.

All the cluster number curves $n_s(t)$ during the time interval $t = 200 - 3400$ s fall onto the

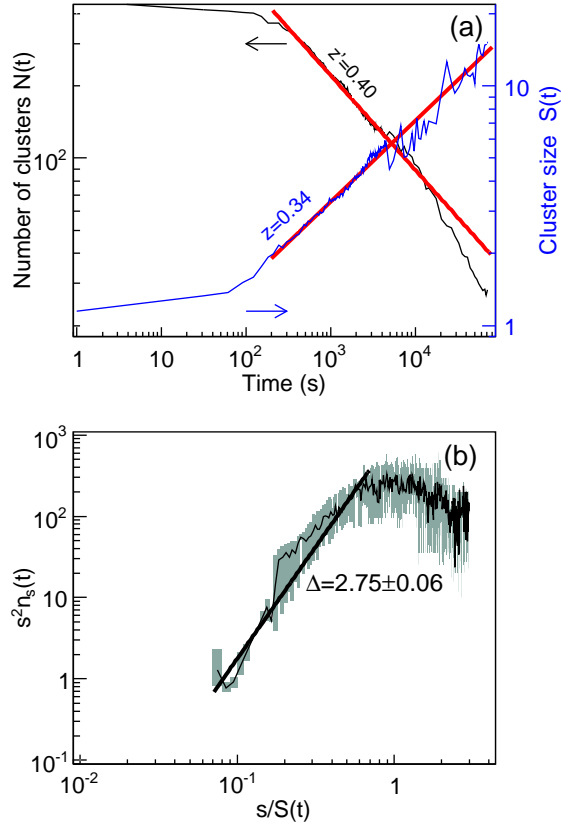


FIG. 4: (color online) (a) The total number of clusters $N(t)$ and the mean (weight average) cluster size $S(t)$ [in units of number of spheres] versus time. (b) The universal scaling function $g(x) \sim x^\Delta$ ($x = s/S(t)$, $x < 1$) calculated for the time interval $t = 200 - 80000$ s.

single curve shown in Fig. 3. From that the characteristic scaling exponent $\Delta = 1.44 \pm 0.08$ was found.

We measured several samples, however, other samples behaved in a different manner. The scaling exponents z , z' , and crossover exponent Δ were different from the results presented above. Typical results for a sample that shows a different type of behaviour are shown in Fig. 4(a). Here the scaling exponents were found to be $z' = 0.40 \pm 0.03$ and $z = 0.34 \pm 0.02$. Similarly to the case discussed above, the cluster numbers $n_s(t)$ ($t = 200 - 80000$ s) that were measured for this sample could be scaled onto a single curve as shown in Fig. 4 (b), but the scaling exponent Δ was nearly twice as large as in the former case, $\Delta = 2.75 \pm 0.06$. Also in this case the visible dynamic behaviour was consistent with diffusion limited cluster-cluster aggregation but with clearly different scaling exponents from those above.

The results presented in Figs. 3 and 4 show that the scaling exponents for this system

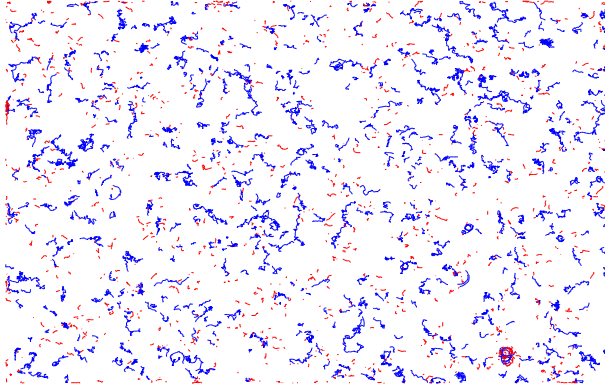


FIG. 5: (color online) Tracks of particles and clusters in the experiment shown in Figs. 2 and 3 during the time interval $t = 0 - 3400$ s. Red lines belong to short tracks that are shorter than 10 time steps (the time step $\Delta t = 30$ s). Blue tracks are longer than 10 time steps. The sample area is about $368 \mu\text{m} \times 274 \mu\text{m}$.

can not be universal. In order to understand this unexpected result we have investigated the motions of individual clusters in more detail.

The complex motion of a cluster was simplified by considering only the motion of its central mass point. There are effects that can change the position of the central mass point with nearly no motion of the cluster as a whole. For example, after joining of two clusters a rearrangement of particles in the new cluster (see the case i) discussed above) takes place. We assume that these disturbing changes are smaller than the influence of random local forces (case iii)) that essentially contribute to the cluster motions. A very slow rotation of a cluster (case ii)) does not change the position of the central mass point.

Cluster tracks shown in Fig. 5 (Fig. 6) were determined for experimental data shown in Fig. 3 (Fig. 4). We see in Figs. 5 and 6 that the clusters moved in two directions, the tracks are complex and show features of Brownian motion as expected.

For Brownian particles it is characteristic that their motion is well described by

$$\langle |\mathbf{r}|^2 \rangle \propto Dt, \quad (3)$$

where \mathbf{r} is the distance vector between an initial position and the position after time t and D is the diffusion coefficient. We checked the validity of Eq. 3 for the cluster tracks and determined the relation $D_s \propto \langle |\mathbf{r}|^2 \rangle / t$ for any cluster of the size s . At each experiment we analyzed about 1000 tracks and found that this equation is valid with a cluster-size

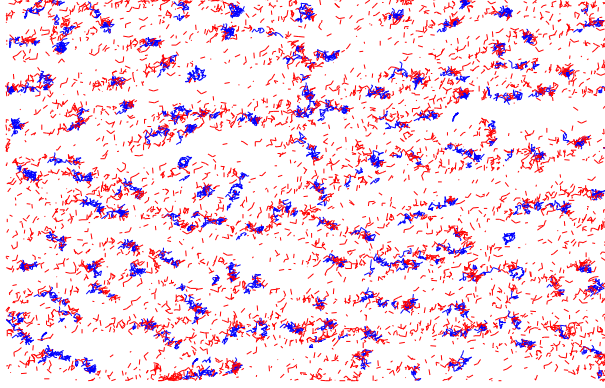


FIG. 6: (color online) Tracks of particles and clusters during aggregation in the time interval $t = 0 - 3400$ s. Red lines belong to short tracks that are shorter than 10 time steps (the time step $\Delta t = 30$ s). Blue tracks are longer than 10 time steps. The sample area is about $368 \mu\text{m} \times 274 \mu\text{m}$.

dependent diffusion coefficient D_s .

We found that D_s clearly depended on the cluster size s as shown in Fig. 7. For the case in Fig. 7 b) the values of the diffusion coefficient D_s fall in a broad range covering nearly three decades. These ranges of values of D_s are significantly larger than possible errors of measurement. An average diffusion coefficient $\langle D_s \rangle$ was calculated for any cluster size s and the results (Fig. 7) were fitted to a scaling law $\langle D_s \rangle \propto s^\gamma$. For the data presented in Figs. 3 and 5 the diffusion scaling exponent $\gamma = -0.62 \pm 0.19$ was found. On the other hand, for the data in Figs. 4 and 6 the diffusion scaling exponent is clearly higher $\gamma = -2.08 \pm 0.51$.

IV. DISCUSSION

We have observed that application of a rotating magnetic field on a 2D magnetic many holes system causes field induced aggregation. The clusters move and can grow in both dimensions, which is different from the case of a constant magnetic field where clusters are free to move in both dimensions but only grow in one dimension as determined by the external magnetic field. The results show that the system is in a nonequilibrium state and its characteristic quantities, number of clusters $N(t)$ and average cluster size $S(t)$, develop and show scaling according to a cluster-cluster aggregation model (**author?**) [2] as was shown in Figs. 3a) and 4a). Both the scaling properties and the broad cluster size distributions found, as well as the existence of a scaling function $g(x)$, are main signatures of cluster-

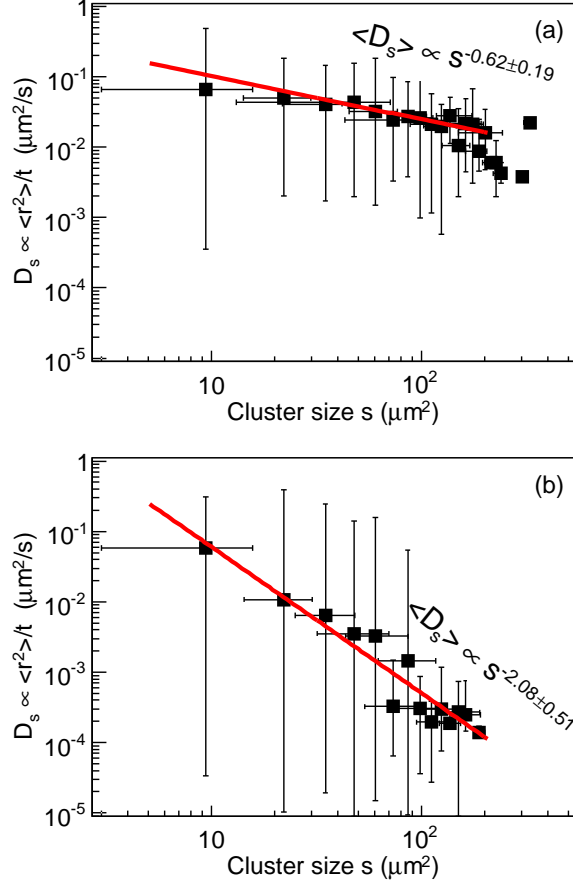


FIG. 7: (color online) The diffusion coefficients vs. cluster size s . (a) For the experimental data shown in Figs. 3 and 5 the diffusion coefficient follows $\langle D_s \rangle \propto s^{-0.62 \pm 0.19}$. (b) For the experimental data shown in Fig. 4 and 6 the diffusion coefficient scales as $\langle D_s \rangle \propto s^{-2.08 \pm 0.51}$.

cluster aggregation and dynamic scaling theory (author?) [4].

In many cases the cluster-cluster aggregation mechanism leads to formation of complex, fractal-like objects (author?) [1]. However, in the present case the structure of the aggregates are simpler with a compact internal organization. In relatively strong magnetic fields, small clusters are regular 2D objects with well ordered structure of the particles inside the clusters. Extremely slow cluster rotations and rearrangement of particles inside the new, bigger clusters have been observed. As a consequence of these effects the clusters are packed into regular objects with a nearly close-packed, triangular structure of the spheres. The cluster diffusion coefficients do not depend on the direction in which the clusters move, i.e., hydrodynamic corrections are not important as they are in case of constant magnetic fields (author?) [9].

In the basic cluster-cluster aggregation model **(author?)** [2] it is assumed that the diffusion coefficient is $\gamma = -1$ and the corresponding scaling exponent is $z = 0.5$. We have determined two distinct values for the diffusion coefficients γ and scaling exponents z as a result of the two clearly different types of behaviour observed in our experiments. The relationship between γ and z for both values of γ follows the equation $z = 1/(1 - \gamma)$ which has been found in other aggregation models. For $\gamma = -0.62 \pm 0.19$ ($\gamma = -2.08 \pm 0.51$) we computed $z = 0.62$ ($z = 0.32$). These scaling exponents agree well with exponents z determined directly from the time dependence of $S(t)$, $z = 0.64 \pm 0.01$ and $z = 0.34 \pm 0.02$, respectively.

Unfortunately, at present we are not able to explain why similar experiments on approximately the same samples (concentrations, layer thickness etc.) show scaling exponents with values that come in two clearly separated ranges and diffusion exponents γ which are different from the expected value $\gamma = -1$. Thus, the scaling exponent z is either clearly lower or higher than the theoretically predicted value $z = 0.5$.

In an earlier study of a similar system of magnetic holes in a constant magnetic fields **(author?)** [8] it was found that for small microspheres (diameters $d = 1.9 - 4.0 \mu\text{m}$ and interaction strength $\lambda = 8 - 370$) the scaling exponents z and z' were approximately equal $z \doteq z'$ and typically slightly lower than 0.5: $0.38 \leq z, z' \leq 0.54$. However, for larger particles, $d = 14 \mu\text{m}$ ($\lambda = 1040 - 10600$) the values of z and z' increased with the value of the dimensionless interaction strength λ from about 0.1 to 0.6, and correspondingly the value of Δ decreased from above 3.0 to ~ 1.5 . Thus, depending on the particle size the scaling exponents changed from being nearly constant and near the theoretically expected values to being strongly non-universal. Although the present particles are within the diameter and λ ranges which showed nearly universal behaviour in Ref. **(author?)** [8], the magnetic interactions are very different (anisotropic in the former and isotropic in the present) and then the range of λ for which the behaviour is non-universal, seems to be changed. It is unclear why the diffusion conditions, as quantified by the values of the diffusion coefficients γ , were so different in the two typical cases reported here. It may possibly be related to fine details in the interaction between the microspheres and the glass plates confining the system. In principle the magnetic holes should be repelled from the confining walls **(author?)** [10] but if for some unknown reason a small fraction of the particles become attracted or even loosely attached to the walls, this would slow down the diffusion as shown by the anomalous

value $\gamma \approx -2$ in one of the analyzed cases. Extremely small values of $\langle D_s \rangle$ could indicate that some of the particles are trapped in the sample volume or on the sample glass boundary.

V. CONCLUSIONS

Diffusion limited cluster-cluster aggregation of magnetic holes has been induced by a rotating magnetic field. The main features of the experimental results are well described by a diffusion limited cluster-cluster aggregation model and dynamic scaling theory. The experimental conditions were designed in effort to have a well defined model of a low concentrated many body system where long range interactions are dominant. At present, the reason why two main aggregation regimes were observed is not clear. This resulted in scaling exponent values clearly different from those predicted by theory for systems with short range interactions. This difference in behaviour was further confirmed by unusual values of the scaling exponent γ of the diffusion coefficient that were found by cluster tracking. An open question remains: Why do the isotropic, long-range particle-particle interactions suppress the diffusion regime where the size-dependence of the diffusion coefficient scales with $\gamma = -1$? This will hopefully be clarified in future studies.

Acknowledgments

The authors thank Arne T. Skjeltorp for many stimulating discussions. The experimental part of this work has been done at the Institute for Energy Technology (IFE, Kjeller). J.C. thanks for kind hospitality at the Physics Department at IFE. Visual data processing was realized using the results of the projects: Negroid and Know ARC. We acknowledge financial support from the Slovak Ministry of Education: Grant. No. 6RP/032691/UPJŠ/08. This work was supported by the Slovak Research and Development Agency under the contract No. RP EU-0006-06.

-
- [1] T. Vicsek, *Fractal Growth Phenomena*, 2nd ed. (World Scientific Singapore, 1992).
 - [2] P. Meakin, *Phys. Rev. Lett.* **51**, 1119 (1983).
 - [3] M. Kolb, R. Bottet, and R. Jullien, *Phys. Rev. Lett.* **51**, 1123 (1983).

- [4] T. Vicsek and F. Family, Phys. Rev. Lett. **52**, 1669 (1984).
- [5] P. Domínguez-García et al, Phys. Rev. E **76**, 051403 (2007).
- [6] G. Helgesen *et al*, Phys. Rev. Lett. **61**, 1736 (1988).
- [7] J. Cernak, J. Magn. Magn. Mater. **132**, 258 (1994).
- [8] J. Černák, G. Helgesen, and A. T. Skjeltorp, Phys. Rev. E **70**,031504 (2004).
- [9] M. C. Miguel and R. Pastor-Satorras, Phys. Rev. E **59**, 826 (1999).
- [10] A. T. Skjeltorp, Phys. Rev. Lett. **51**, 2306 (1983).
- [11] G. Helgesen, P. Pieranski, and A. T. Skjeltorp, Phys. Rev. Lett. **64**, 1425 (1990).
- [12] P. Pieranski, S. Clausen, G. Helgesen, and A. T. Skjeltorp, Phys. Rev. Lett. **77**, (1996).
- [13] R. Toussaint *et al*, Phys. Rev. E **69**, 011407 (2004).
- [14] P. Tierno, R. Muruganathan, and T. M. Fisher, Phys. Rev. Lett. **98**, 028301 (2007).
- [15] Type EMG 909, produced by Ferrotech, Nashua, New Hampshire.